Hepatology Research

Hepatology Research 2014; 44: 700–706 doi: 10.1111/hepr.12163

Case Report

Early venous return in hepatic angiomyolipoma due to an intratumoral structure resembling an arteriovenous fistula

Yasuhito Iwao,[1,3] Hidenori Ojima,[4] Hiroaki Onaya,[2] Yoshihiro Sakamoto,[3] Yoji Kishi,[3] Satoshi Nara,[3] Minoru Esaki,[3] Yasunori Mizuguchi,[2] Masahiko Ushigome,[1] Daisuke Asahina,[1] Nobuyoshi Hiraoka,[4] Kazuaki Shimada,[3] Tomoo Kosuge[3] and Yae Kanai[4]

[1]*Pathology Division,* [2]*Diagnostic Radiology Division,* [3]*Hepato-biliary and Pancreatic Surgery Division, National Cancer Center Hospital, and* [4]*Division of Molecular Pathology, National Cancer Center Research Institute, Tokyo, Japan*

Early venous return (EVR) is an important radiological feature of hepatic angiomyolipoma (HAML) that can aid in differential diagnosis, but the pathogenic mechanisms of EVR have yet to be elucidated. We present the first HAML case for which a probable mechanism for EVR is described. The patient was a 46-year-old woman, who had a growing 6-cm tumor with EVR in segment 3 of the liver as revealed by dynamic contrast-enhanced computed tomography. Left hepatic lobectomy was performed to prevent tumor rupture. Histopathological and immunohistochemical analyses of the excised tumor indicated HAML. Successive microsections of the tumor were stained with hematoxylin–eosin and Victoria blue to visualize the vascular structure within and around the tumor. These analyses led to three major findings. First, many well-defined thick-walled vessels, such as arteries, were found entering the tumor. Second, many thick-walled vessels within the tumor were connected directly to thin-walled vessels, resembling arteriovenous fistulae. Finally, thin-walled intratumoral vessels were connected directly to the hepatic vein. These histological findings suggested that the rich arterial flow into the tumor was being rapidly drained into the hepatic vein through intratumoral arteriovenous connections. We also detected these same anomalous circulatory pathways in tissue sections from three of four additional HAML cases with EVR. Aberrant arteriovenous fistulae within the tumor may account for many cases of EVR in HAML patients.

Key words: angiomyolipoma, arteriovenous fistula, diagnostic imaging, hemodynamics, liver neoplasm, surgical pathology

INTRODUCTION

ANGIOMYOLIPOMA IS A rare tumor that most often arises in the kidney or liver.[1] Since the first discovery of hepatic angiomyolipoma (HAML) by Ishak in 1976,[2] over 200 cases have been reported worldwide.[1] Renal angiomyolipoma may lead to tuberous sclerosis, whereas HAML does not.[3] Recent genetic analysis of HAML has shown that it is a true benign mesenchymal tumor.[4] Nonetheless, HAML should be accurately diagnosed and closely monitored as some cases show malignant transformation.[1,4–7] Yang *et al.* suggested conservative management of HAML even in asymptomatic patients if they meet the following criteria: (i) tumor size smaller than 5 cm; (ii) angiomyolipoma confirmed through fine-needle aspiration biopsy; (iii) patients with good treatment compliance; and (iv) negative for the hepatitis virus.[1]

Angiomyolipoma is characterized by a heterogeneous mixture of smooth muscle cells, mature adipose tissue and thick-walled blood vessels.[8,9] It is not difficult to diagnose pathologically by immunoreactivity to antibodies against HMB-45 and α-smooth muscle actin (α-SMA).[9] However, it can be difficult to diagnose clinically because the variable admixtures of smooth muscle, adipose tissue and blood vessels confer a variety of imaging presentations that can resemble other pathologies.[10] It is especially important to differentiate HAML from hepatocellular carcinoma (HCC) because these pathologies have similar radiological features but markedly different prognoses. Several recent reports using

Correspondence: Dr Hidenori Ojima, Division of Molecular Pathology, National Cancer Center Research Institute, 5-1-1 Tsukiji, Chuo-ku, Tokyo 104-0045, Japan. Email: hojima@ncc.go.jp
Received 18 November 2012; revision 4 May 2013; accepted 12 May 2013.

dynamic contrast-enhanced computed tomography (CT) have suggested that early opacification of the HAML drainage vein, or early venous return (EVR, also termed early venous drainage) is a useful feature for distinguishing HAML from HCC.[11–14] However, no previous reports have investigated the mechanism of EVR in HAML. We present the first HAML case in which EVR is explained mechanistically by formation of intratumoral arteriovenous connections and drainage of intratumoral veins into the hepatic vein. Moreover, histopathological analysis of other resected samples from our institute indicated this aberrant vascular pattern in three of four additional cases of HAML with EVR.

CASE REPORT

A 46-YEAR-OLD WOMAN was diagnosed with a hepatic mass during a routine health check-up 2 years prior. Blood examinations revealed no abnormalities; however, the first abdominal ultrasonography (US) when she was 44 years old revealed a round, well-demarcated, 4-cm mass in segment 3 of the liver showing a heterogenic high echo. Contrast-enhanced US with galactose microparticles initially showed tumor vessels followed by complete tumor enhancement in the early arterial phase and staining of the whole tumor parenchyma as well as the surrounding liver in the late vascular phase (5 min later).

Unenhanced CT showed a hypoattenuated lesion relative to the liver parenchyma (Fig. 1a). Dynamic contrast-enhanced CT demonstrated heterogeneous tumor hyperattenuation in the arterial phase, heterogeneous iso-attenuation in the portal venous phase and hypoattenuation in the equilibrium phase with an irregular shape (Fig. 1b–d). Contrast-enhanced CT scans obtained during the arterial phase also showed early opacification of the left hepatic vein (Fig. 1b), suggesting early drainage within the tumor because at this time point, the right and middle hepatic veins were not opacified.

The tumor was hyperintense on T_2-weighted fast-spin echo magnetic resonance images and hypointense on T_1-weighted spin-echo images. No fat component was detected in the lesion, even on T_1-weighted in-phase or out-of-phase gradient-echo images.

We diagnosed this tumor as HAML with a minimal fat component. During follow up 19 months after initial presentation, when the patient was 46 years old, the tumor size was confirmed to be 6 cm, and we planned to conduct angiography for differential diagnosis. Proper hepatic arteriography, which had no vascular anomaly and no iatrogenic artifacts, revealed a large hypervascular tumor with prominent vascular structures and early returning veins connecting to the left hepatic vein. Single-level dynamic CT during hepatic arteriography (CTHA) showed extremely marked hyperattenuation in the tumor, followed by early hypoattenuation in the left hepatic lobe compared to the right lobe. The drainage vein of the tumor connecting to the left hepatic vein was opacified earlier than the middle and right hepatic veins (Fig. 1e–h, see Video 1, Supporting Information, which demonstrates single-level dynamic CTHA). A CT scan of the entire liver during hepatic arteriography revealed a hypervascular main tumor and hypoattenuation of the surrounding left lobe. The left lobe also exhibited three new smaller hypervascular nodules, two of which were located in segment 4 and the other in segment 2 (Fig. 1i). CT during arterial portography revealed no difference in attenuation between the right and left lobes, whereas the main tumor and the three nodules were hypoattenuated relative to the surrounding liver (Fig. 1j).

We suspected that the main lesion was a malignant tumor, such as HAML with malignant change or HCC, because of the appearance of three new hypervascular nodules. It was judged that this tumor could rupture if left untreated, and therefore, we performed left hepatic lobectomy.

Pathological findings

The main tumor in segment 3 was a 6-cm elastic soft tumor that appeared to protrude from the hepatic serosa. The cut surface of a fresh tumor specimen was yellowish with no capsule and a small amount of hemorrhage (Fig. 1k). Three whitish nodules were found, measuring 7 mm and 4 mm in segment 4 and 3 mm in segment 2 (Fig. 1k). Histologically, the main tumor comprised adipose tissue, sheets of tumor cells with rich eosinogranular cytoplasm, and irregular vessels. The tumor cells were immunoreactive to antibodies against α-SMA (dilution 1:100; Dako, Glostrup, Denmark) and HMB-45 (dilution 1:10; Dako), confirming HAML (Fig. 2a–c). The three satellite nodules were composed of hyperplastic hepatocytes with proliferating bile ductules and thick-walled arteries, suggesting focal nodular hyperplasia (FNH) (Fig. 2d).

Radiological–pathological correlation

To investigate the pathological mechanism of EVR, 60 successive microsections, one for every 3 μm of HAML thickness, were prepared and stained with

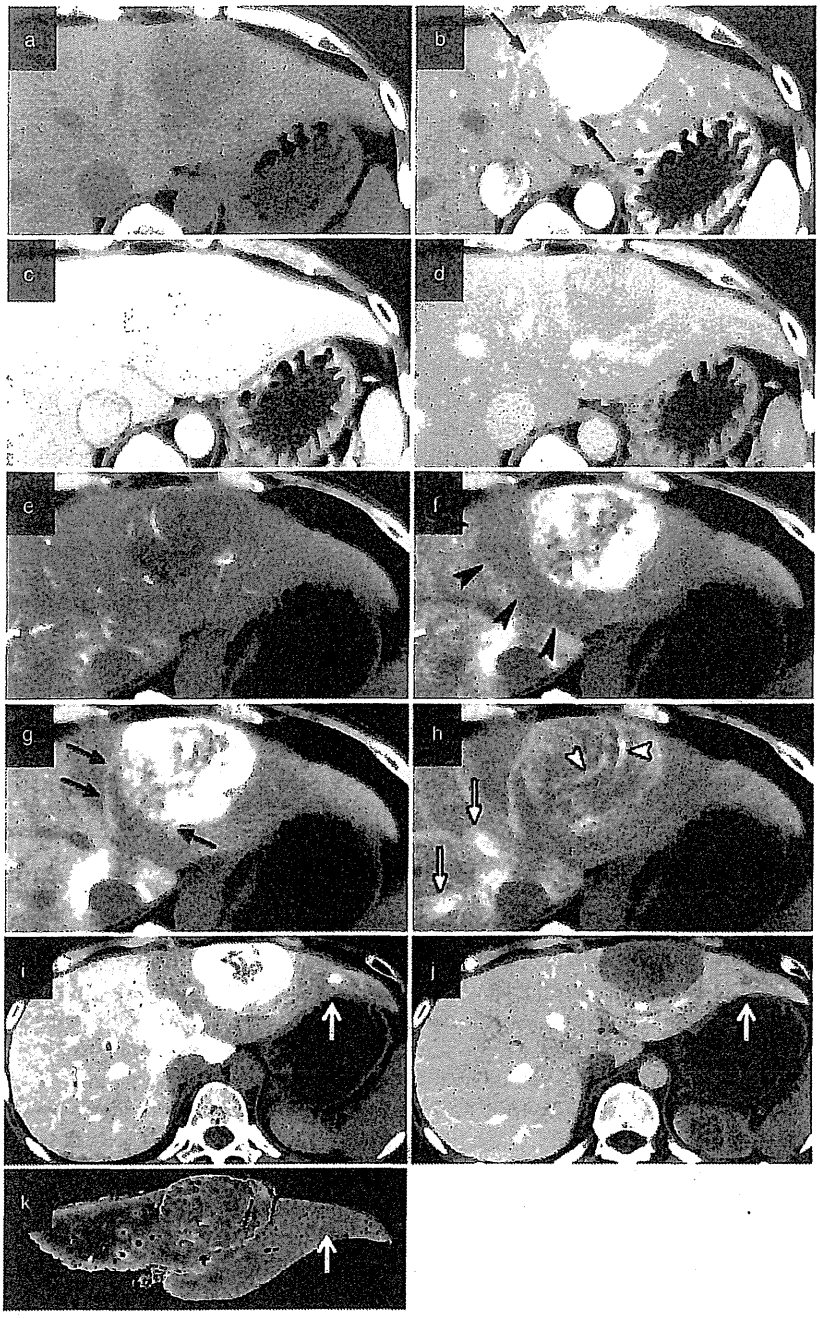

Figure 1 Images of the tumor acquired during the first examination. (a) Unenhanced computed tomography (CT) showing a hypoattenuated lesion relative to the surrounding liver. (b) Contrast-enhanced CT obtained during the arterial phase showing a markedly hyperattenuated mass with early venous return (arrows). (c) In the portal venous phase, the mass exhibits heterogeneous iso-attenuation. (d) In the equilibrium phase, the mass exhibits hypoattenuation. Single-level dynamic CT during hepatic arteriography (see Video 1, Supporting Information, which demonstrates the entire procedure). (e) Tiny vessels are evident in the tumor periphery at 4 s. (f) The main tumor shows strong heterogeneous enhancement, and attenuation of the left lobe (bearing the tumor) is lower than that of the right lobe at 6 s (black arrowheads). (g) Two early draining veins connecting to the left hepatic vein can be seen at 8 s (black arrow). (h) Tortuous veins are evident within the tumor (white arrowheads). Opacification of the middle and right hepatic veins can be seen at 15 s (white arrows). (i) CT during hepatic arteriography shows a hypervascular main lesion and one of three other small hypervascular lesions (arrow) in the left lobe. Attenuation of the left lobe is lower than that of the right lobe. (j) On CT during arterial portography, the large lesion shows a portal perfusion defect and the small lesion (arrow) shows decreased portal perfusion. Note iso-attenuation of the left and right lobes, indicating normal portal venous flow in both lobes. (k) Cut surface of the resected specimen corresponding to the CT slice. The main tumor contains scattered hemorrhagic foci. This section also captures one of the three small lesions (arrow) seen on CT.

hematoxylin–eosin and Victoria blue (HE-VB) for histological identification of the intratumoral vessels. Many thick-walled vessels composed of elastic fibers and stained with VB were observed around Glisson's capsule in the tissue adjacent to the HAML. Successive microsections revealed that these peripheral thick-walled vessels were probably arteries entering the HAML (Fig. 3a–c; see Video 1, Supporting Information), but with no corresponding veins (termed unpaired arteries in the peripheral tumor [UAPT]). Within HAML were many

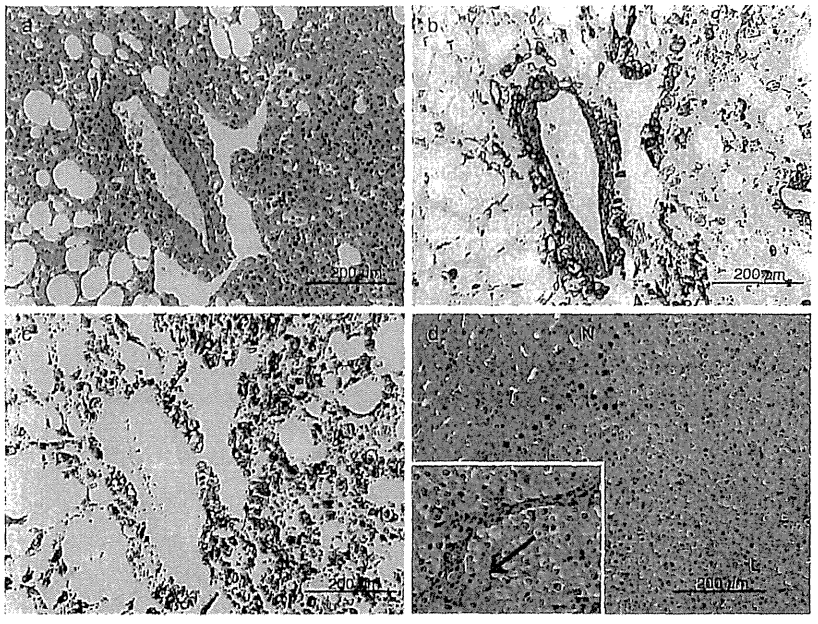

Figure 2 (a) Microscopic features of the main tumor, including many thick-walled vessels resembling "unpaired arteries", thin-walled vessels such as veins, adipose tissue and smooth muscle (hematoxylin–eosin [HE]). (b) α-Smooth muscle actin (SMA). (c) HMB-45. (d) Microscopic features of the small peripheral lesions demonstrate clear demarcation (dotted line), degenerative muscular arteries (arrow) and proliferation of bile ductules in a fibrosis stroma without portal veins (inset) (HE). Scale bar, 200 μm. (d) The dotted line represents the boundary between the lesion (L) and non-lesion (N).

thin-walled vessels, dilated, sinusoid-like vessels, and thick-walled vessels, resembling arteries, connected directly by structures resembling arteriovenous fistulae (SRAVF) (Fig. 3d–f, see Video 1, Supporting Information). These abnormal thin-walled vessels were also connected directly to the extratumoral hepatic vein in the surrounding liver (Fig. 3g–i, see Video 1, Supporting Information), which we termed "connections of tumor vessels with the hepatic vein" (CTVHV). In addition, there were many dilated hepatic veins around the HAML.

Review of HAML cases in a single institution

Since 2001, four other cases of HAML were treated by surgical resection in our hospital. In three of these four cases, EVR was detected in the arterial phase of contrast-enhanced CT (Fig. 4, See Video 2, Supporting Information). For each case, we tried to find the three major pathological characteristics UAPT, SRAVF and CTVHV in HE-stained sections (Fig. 4). UAPT and CTVHV were found in all cases. Furthermore, SRAVF were found in cases 2, 3 and 4, but these structure were absent in case 5. Cases 2 and 3 also exhibited many dilated hepatic veins around HAML.

DISCUSSION

ONLY 10 CASES of HAML with EVR have been reported in English-language published work.[10–14] Only one previous case report has discussed the reasons for EVR in HAML based solely on radiological findings, which included the presence of a dilated intratumoral central vessel and connection of this vessel directly with the extratumoral hepatic vein.[10] However, no previous study has correlated imaging results with high-resolution tumor histopathology.

The three unique features, such as UAPT, SRAVF and CTVHV of the tumor circulation, were revealed by histopathological analysis in both the primary study case (case 1) and three of the four additional cases of HAML with EVR resected at our institution. The only exception was case 5, a patient with a 20-mm tumor and no detectable SRAVF. This result suggested that in most cases of HAML with EVR, there are aberrant changes in hemodynamics. Rich arterial flow through thick-walled vessels entering the tumor (which can be regarded as equivalent to "unpaired arteries" in HCC) indicate that most HAML tumors are markedly hypervascular. However, blood is rapidly drained into the hepatic vein through abnormal arteriovenous connections resembling arteriovenous fistulae (AVF), resulting in EVR observed in the arterial phase of dynamic contrast-enhanced CT.

The fifth case of HAML showed no SRAVF. Because the density of thick-walled blood vessels is different in each tumor, we could not measure the proportion of SRAVF. HAML is characterized by a heterogeneous mixture of smooth muscle cells, mature adipose tissue and thick-walled blood vessels, with a region of thick-walled

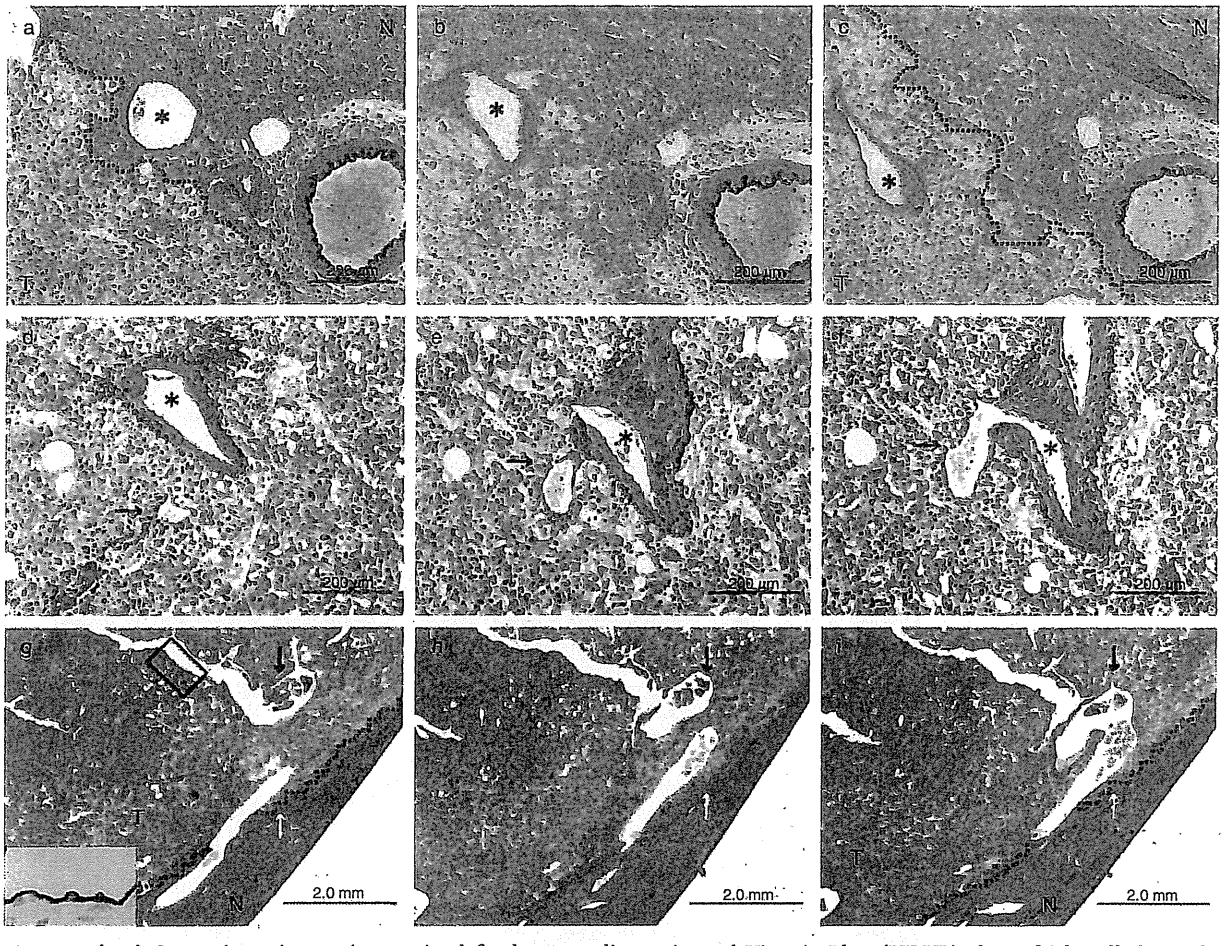

Figure 3 (a–c) Successive microsections stained for hematoxylin–eosin and Victoria Blue (HE-VB) show thick-walled vessels resembling arteries (*) entering the hepatic angiomyolipoma (HAML) from near the normal Glisson's capsule (scale bar, 200 μm). (d–f) Thick-walled vessels (*) connect with thin-walled vessels (arrow) in the HAML (HE-VB staining; scale bar, 200 μm). (g–i) Thin-walled vessels connect directly with the hepatic vein (white arrow) outside the HAML (HE-VB staining; scale bar, 2 mm). (g) Inset (higher magnification view of squared section). CD31 expression detected by anti-CD31 antibody in the endothelial cells of the vessel area is shown (also see Video 1, Supporting Information). These three series of microsections were independent vessels. (a,c,g,i) The dotted line represents the boundary between the tumor (T) and surrounding normal tissue (N).

blood vessels and SRAVF. Moreover, HAML was reported to have a rich network of capillaries throughout,[8] therefore, we considered the possibility that part of the capillary network was connected to CTVHV through a sinus in case 5.

These abnormal hemodynamic features of HAML clearly differ from those of HCC, even though the latter lesions appear hypervascular in the arterial phase of dynamic contrast-enhanced CT and also show many unpaired arteries on histology.[15] However, connections that resemble AVF are not observed in HCC, and drainage to the portal vein occurs in the portal phase rather than the arterial phase of dynamic contrast-enhanced CT or CTHA, creating a so-called "corona enhancement of the adjacent liver".[16] These differences in vascular structures between HAML and HCC make EVR a very useful feature for differentiating these two tumors.

The left hepatic lobe with HAML in this case showed arterial hypoperfusion abnormality on CTHA, whereas portal flow did not change on CT arterial portography. We speculate that the change in the hemodynamics of the left lobar distribution, relative to the decrease in

Case No.	Age (y.o.) Sex	Location Size	EVR	UAPT	SRAVF	CTVHV
1	40 F	S2 60 mm	Present case			
2	31 F	S3 75 mm	+	+	+	+
3	58 M	S2 50 mm	+	+	+	+
4	41 F	S3 40 mm	+	+	+	+
5	56 M	S6 20 mm	−	+	Not found	+

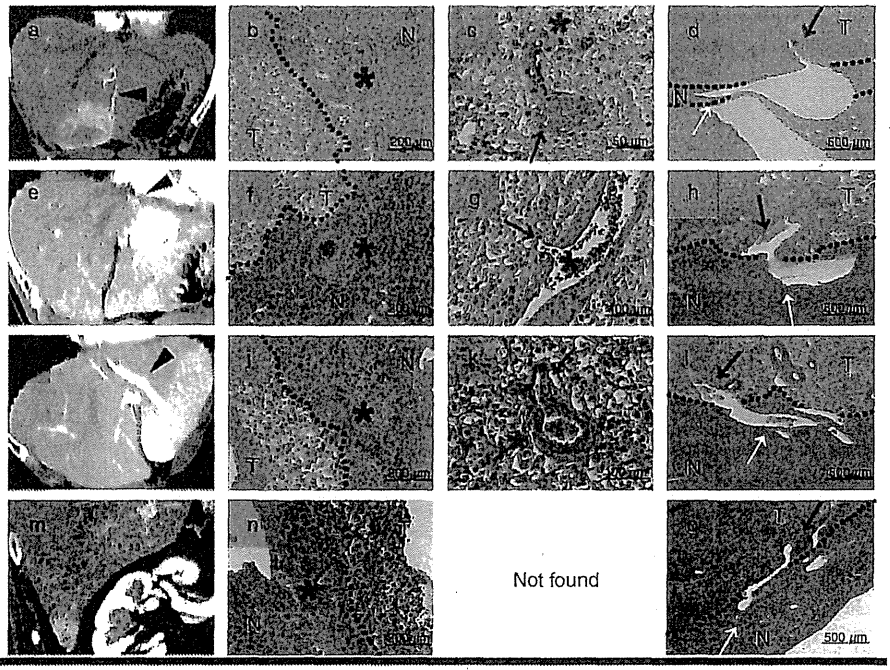

Figure 4 Summary of five resected hepatic angiomyolipoma (HAML) cases in our institution since 2001. Contrast-enhanced computed tomography images during the arterial phase in case 2 (a), 3 (e), 4 (i) and 5 (m) are shown. Early venous return (EVR) (arrowhead) is observed in cases 2, 3 and 4, but not in case 5. Microsections stained by hematoxylin–eosin are also shown. All cases exhibit unpaired arteries (*) in the peripheral HAML ([b,f,j,n] scale bar, 200 μm). All cases except case 5 also show intratumoral connections of thick-walled vessels (*) to thin-walled vessels (black arrow) or dilated sinusoidal vessels resembling arteriovenous fistulae ([c] scale bar, 50 μm; [g,k] scale bar, 100 μm). All four cases exhibit intratumoral vessels connected to the hepatic vein (white arrow) ([d,h,l,o] scale bar, 500 μm). (b,d,f,h,j,l,n,o) The dotted line represents the boundary between the tumor (T) and surrounding normal tissue (N). CTVHV, connection of the tumor vessel and hepatic vein; F, female; M, male; SRAVF, structure resembling arteriovenous fistula; UAPT, unpaired artery in the peripheral tumor.

arterial flow, is associated with the hemodynamics of HAML. This finding was apparent because the tumor was originally markedly hypervascular and sufficiently large to demonstrate the lobar attenuation difference by the steal phenomenon (the siphoning effect). The phenomenon of "hypoattenuated areas adjacent to the hypervascular tumor" is also known as findings of a transient hepatic attenuation difference of lobar or segmental distribution in the arterial phase of intravenous dynamic contrast-enhanced CT in some cases with hypervascular hepatic tumors (large cavernous hemangiomas, FNH, hepatic adenomas).[17,18]

We also found multiple, mainly solitary, FNH in the left hepatic lobe bearing the HAML in case 1. Some reports have described a relationship between hyperplastic lesions, such as FNH or FNH-like lesions, and abnormal hepatic hemodynamics.[9,19] Thus, these multiple FNH might have resulted from aberrant vascular remodeling. We speculate that the abnormal hemodynamics of HAML, revealed by both radiology and histopathology, caused EVR, the hepatic attenuation difference in the left hepatic lobe and multiple FNH.

In summary we report the first case of EVR in HAML for which the histopathological mechanisms were clarified by *in vivo* imaging and histopathological analysis of the resected tumor. We demonstrate that arteriovenous shunting within the HAML can account for EVR, an important clinical feature that allows differentiation of HAML from HCC.

ACKNOWLEDGMENT

THIS WORK WAS supported in part by the National Cancer Center Research and Development Fund (23-A-35).

REFERENCES

1 Yang CY, Ho MC, Jeng YM *et al.* Management of hepatic angiomyolipoma. *J Gastrointest Surg* 2007; **11**: 452–7.
2 Ishak KG. Mesenchymal tumors of the liver. In: Okuda K, Peters RL, eds. *Hepatocellular Carcinoma*. New York: Wiley Medical, 1976; 247–307.
3 Stillwell TJ, Gomez MR, Kelalis PP *et al.* Renal lesions in tuberous sclerosis. *J Urol* 1987; **138** (3): 477–81.
4 Flemming P, Lehmann U, Becker T *et al.* Common and epithelioid variants of hepatic angiomyolipoma exhibit clonal growth and share adistinctive immunophenotype. *Hepatology* 2000; **32**: 213–7.
5 Dalle I, Sciot R, de Vos R *et al.* Malignant angiomyolipoma of the liver: a hitherto unreported variant. *Histopathology* 2000; **36**: 443–50.
6 Croquet V, Pilette C, Bouju B *et al.* Late recurrence of a hepatic angiomyolipoma. *Eur J Gastroenterol Hepatol* 2000; **12**: 579–82.
7 Parfitt JR, Bella AJ, Izawa JI *et al.* Malignant neoplasm of perivascular epithelioid cells of the liver. *Arch Pathol Lab Med* 2006; **130**: 1219–22.
8 Ishak KG, Goodman ZD, Stocker JT. *Atlas of Tumor Pathology, Tumors of the Liver and Intrahepatic Bile Ducts*. Washington, DC: Armed Forces Institute of Pathology, 2001; 99–108.
9 Bosman FT, Carneiro F, Hruban RH *et al. WHO Classification of Tumours of the Digestive System*. Lyon: IARC Press, 2010; 244–5, 254–61.
10 Sakamoto Y, Inoue K, Ohtomo K *et al.* Magnetic resonance imaging of angiomyolipoma of the liver. *Abdom Imaging* 1998; **23**: 158–60.
11 Murakami T, Nakamura H, Hori S *et al.* Angiomyolipoma of the liver. Ultrasound, CT, MR imaging and angiography. *ACTA Radiol* 1993; **34**: 392–4.
12 Yoshimura H, Murakami T, Kim T *et al.* Angiomyolipoma of the liver with least amount of fat component: imaging features of CT, MR, and angiography. *Abdom Imaging* 2002; **27**: 184–7.
13 Zheng RQ, Kudo M. Hepatic angiomyolipoma: identification of an efferent vessel to be hepatic vein by contrast-enhanced harmonic ultrasound. *Br J Radiol* 2005; **78**: 956–60.
14 Jeon TY, Kim SH, Lim HK *et al.* Assessment of triple-phase CT findings for the differentiation of fat-deficient hepatic anagiomyolipoma from hepatocellular carcinoma in non-cirrhotic liver. *Eur J Radiol* 2010; **73**: 601–6.
15 Ueda K, Terada T, Nakanuma Y *et al.* Vascular supply in adenomatous hyperplasia of the liver and hepatocellular carcinoma: a morphometric study. *Hum Pathol* 1992; **23**: 619–26.
16 Ueda K, Matsui O, Kawamori K *et al.* Hypervascular hepatocellular carcinoma: evaluation of hemodynamics with dynamic CT during hepatic arteriography. *Radiology* 1998; **206**: 161–6.
17 Itai Y, Moss AA, Goldberg HI. Transient hepatic attenuation difference of lobar or segmental distribution detected by dynamic computed tomography. *Radiology* 1982; **144**: 835–9.
18 Colagrande S, Carmignani L, Pagliari A *et al.* Siphoning effect and steal phenomenon combined to focal hepatic lesions on spiral CT. Four cases report. *Radiol Med* 2002; **102**: 267–74.
19 Kondo F, Koshima Y, Ebara M. Nodular lesions associated with abnormal liver circulation. *Intervirology* 2004; **47**: 277–87.

SUPPORTING INFORMATION

ADDITIONAL SUPPORTING INFORMATION may be found in the online version of this article at the publisher's web-site:

Supporting Information. Video 1 demonstrates single-level dynamic computed tomography during hepatic arteriography and successive microsections showing the three vascular features of hepatic angiomyolipoma with early venous return.
Supporting Information. Video 2 shows contrast-enhanced computed tomography during the arterial phase of cases 2, 3, 4 and 5.
Supporting Information. Digital subtraction angiography (DSA) from proper hepatic artery (PHA).

Original article

Right portal vein embolization with absolute ethanol in major hepatic resection for hepatobiliary malignancy

K. Sofue[1,3], Y. Arai[1], K. Shimada[2], Y. Takeuchi[1], T. Kobayashi[4], M. Satake[4] and K. Sugimura[3]

Divisions of [1]Diagnostic Radiology and [2]Hepatobiliary and Pancreatic Surgery, National Cancer Centre Hospital, Tokyo, [3]Department of Radiology, Kobe University, Graduate School of Medicine, Kobe, and [4]Department of Radiology, National Cancer Centre Hospital East, Kashiwa, Japan
Correspondence to: Dr K. Sofue, Division of Diagnostic Radiology, National Cancer Centre Hospital, 5-1-1, Tsukiji, Chuo-ku, Tokyo 104-0045, Japan (e-mail: keitarosofue@yahoo.co.jp)

Background: This study aimed to evaluate the safety and efficacy of preoperative right portal vein embolization (PVE) with absolute ethanol in patients with hepatobiliary malignancies.

Methods: PVE was performed via a percutaneous transhepatic ipsilateral approach, and the right portal branch was embolized with absolute ethanol. Technical success and complications following PVE, and changes in liver enzyme levels were evaluated. Changes in future liver remnant (FLR) and FLR/total functional liver volume ratio were calculated. Complications following hepatic resection were assessed.

Results: A total of 83 patients with hepatobiliary malignancies (53 men, 30 women; mean age 68 years) underwent right PVE. Tumour types were hilar cholangiocarcinoma (37), liver metastases (14), gallbladder cancer (13), intrahepatic cholangiocellular carcinoma (10) and hepatocellular carcinoma (HCC) (9). PVE was performed successfully in all patients. Four patients (5 per cent) developed complications following PVE (liver abscess 2, left portal vein thrombosis 1, pseudoaneurysm 1), but this did not preclude hepatic resection. Liver enzyme levels rose transiently after PVE. The mean FLR and FLR/total functional liver volume increased after PVE (from 366 to 513 cm^3 and from 31 to 43 per cent respectively; both $P < 0{\cdot}001$). Changes in the FLR and FLR/total functional liver volume ratio were comparable between patients with HCC and those with other malignancies (42 and 44 per cent, and 12 and 12 per cent, respectively). Sixty-nine of 83 patients underwent hepatic resection at a median of 25 days after PVE, with no postoperative mortality.

Conclusion: Preoperative right PVE with absolute ethanol is safe and effective for induction of selective hepatic hypertrophy in patients with hepatobiliary malignancy.

Paper accepted 26 March 2014
Published online 11 June 2014 in Wiley Online Library (www.bjs.co.uk). **DOI:** 10.1002/bjs.9541

Introduction

Percutaneous transhepatic portal vein embolization (PVE) has gained acceptance in the preoperative treatment of selected patients who are potential candidates for major hepatic resection[1–3]. PVE leads to atrophy of the embolized lobe and compensatory hypertrophy of the future liver remnant (FLR). This reduces the risk of postoperative hepatic failure in patients undergoing major hepatic resection[4–7].

The degree and rate of hypertrophy of the non-embolized liver segments depend on many factors, such as underlying liver disease, presence of diabetes mellitus, initial FLR volume and embolic materials used. Various commercially available embolic materials, including gelatin sponge, fibrin glue, cyanoacrylate and ethiodized oil, polyvinyl alcohol particles and absolute ethanol, have been used for PVE[1,2,6,8–10]. Ideally, embolic materials for PVE should cause complete and permanent occlusion of the portal vein with minimal risk of recanalization, and should be readily available and easily administered.

Absolute ethanol is a reliable embolic material owing to its strong coagulative effect and the low risk of recanalization following its use. Its embolic mechanism and histopathological changes in the embolized liver have been addressed in experimental studies[11–13]. Absolute ethanol has the advantages of being readily available, cheap and easily administered owing to its low viscosity. Although the hypertrophy rate has been shown to be greater with ethanol than with other embolic materials, and absolute ethanol may be particularly useful in patients with hepatocellular carcinoma (HCC)[10,14–16], few studies have reported on the

value of absolute ethanol for preoperative PVE[17]. Equally, the safety and efficacy of absolute ethanol for right PVE in patients with hepatobiliary malignancy undergoing major hepatic resection have not been elucidated fully.

The purpose of this study was to evaluate the safety and efficacy of right portal vein embolization with absolute ethanol before major hepatic resection for hepatobiliary malignancy.

Methods

All patients with advanced hepatobiliary malignancy, who underwent preoperative right PVE between April 2007 and December 2011 at the authors' institution to increase the volume of an insufficiently small left FLR before surgery, were enrolled. Written informed consent was obtained from all patients. In principle, PVE was indicated when the FLR was estimated to be less than 40 per cent in patients whose indocyanine green retention rate at 15 min was less than 15 per cent[17]. When patients were jaundiced owing to biliary obstruction, percutaneous or endoscopic biliary drainage of the left FLR was carried out.

Procedures

All PVEs were done as an inpatient procedure under local anaesthesia with 1 per cent lidocaine, and conscious sedation with an intramuscular injection of 15 mg pentazocine and 50 mg hydroxyzine hydrochloride. Intravenous broad-spectrum antibiotics were administered prophylactically 6 h before the procedure in all patients and continued for up to 3 days afterwards.

A peripheral portal venous branch was accessed percutaneously and transhepatically through the side to be resected (ipsilateral approach) with a 21-G needle (Top, Tokyo, Japan) under ultrasonographic guidance. A 5-Fr sheath (introducer set; Medikit, Tokyo, Japan) was then introduced into the portal vein using the Seldinger technique under fluoroscopic guidance. Digital subtraction portography was used to identify the portal venous anatomy through a 5-Fr angiographic pigtail catheter in the main portal trunk (*Fig. 1a*).

After selective right anterior and posterior portography with balloon occlusion using a reverse-curved 5-Fr balloon catheter with a tip hole (Selecon balloon catheter; Terumo Clinical Supply, Gifu, Japan) (*Fig. 1b,c*), absolute ethanol was bolus-injected into the right anterior and right posterior branch. The amount injected (99·5 per cent ethanol; Fuso Pharmaceutical Industries, Osaka, Japan) was equivalent to the amount of contrast material injected on portography. The balloon was kept inflated for 10 min to block the embolized branches and prevent reflux of ethanol. Some 15 mg pentazocine was administered intravenously if the patient complained of severe pain. With the balloon deflated slightly, a small amount of contrast material was administered to confirm complete embolization of portal venous branches, after which the balloon was deflated completely. If active flow was still observed, additional absolute ethanol was injected.

After embolization, the balloon catheter was flushed carefully in the right portal venous branch and portography then carried out via the main portal trunk (*Fig. 1d*). Subsequently, the tract of the liver through which the sheath was introduced was embolized with 3–5-mm stainless steel coils (MReye® embolization coil; William Cook, Bjaeverskov, Denmark). Portal venous pressure was not measured before or after PVE, because no patient had a history of portal hypertension. Patients were allowed 2 h of bed rest after the procedure. Patients underwent Doppler ultrasonography 1 day later to verify successful embolization. They were discharged when clinically stable and had no complaints (3–5 days after the procedure).

Follow-up examination

In all patients, serum levels of aspartate aminotransferase, alanine aminotransferase, lactate dehydrogenase, alkaline phosphatase and total bilirubin were assessed before PVE, on the first 1 or 2 days after PVE and just before hepatic resection.

Contrast-enhanced computed tomography (CT) was performed before PVE and shortly before hepatic resection. Transverse CT images were obtained with a multidetector row helical CT unit (Aquilion™; Toshiba Medical Systems, Tokyo, Japan) that had 16 detector rows. After intravenous contrast injection, portal phase images were acquired from the dome to the inferior part of the liver with a section thickness of 5 mm. Images were reviewed on a 1536×2048 picture archiving and communication systems (PACS) monitor (Radi CS; Nihon IBM, Tokyo, Japan), and operator-defined handheld regions of the total liver volume, liver tumour volume and FLR volume (segments II–IV) were measured at a workstation by an interventional radiologist and the referring surgeon. Volumes were calculated automatically by multiplying the area in each image by interval thickness and by adding all interval volumes of each part. Total functional liver volume was defined as total liver volume minus tumour volume, and FLR/total functional liver volume ratio was calculated before and after PVE.

Surgical resection was carried out after review of the patient's clinical status and CT findings, by one of four surgeons[6,17]. If disease progression was documented at CT after PVE, or distant metastasis or peritoneal

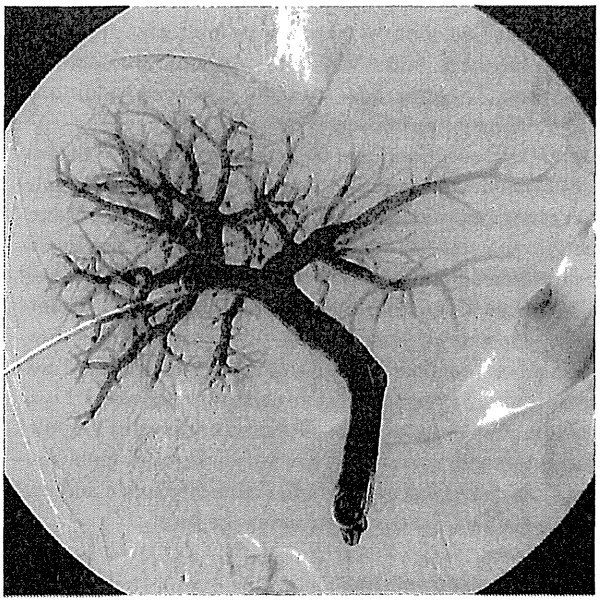

a Before portal vein embolization

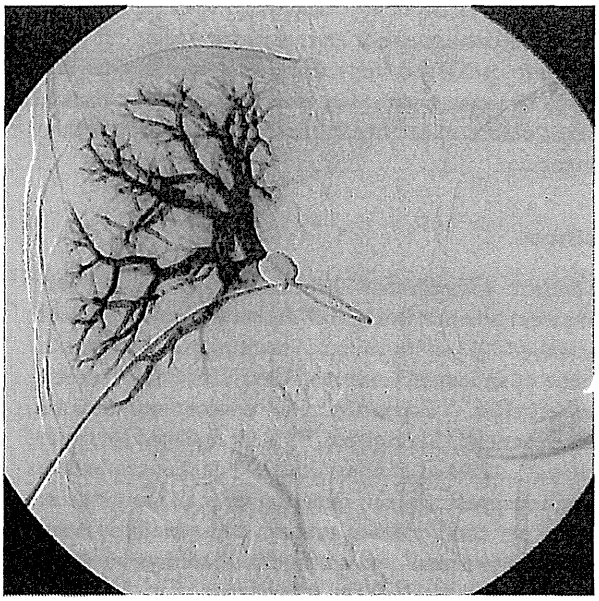

b Balloon occlusion before ethanol injection, right anterior view

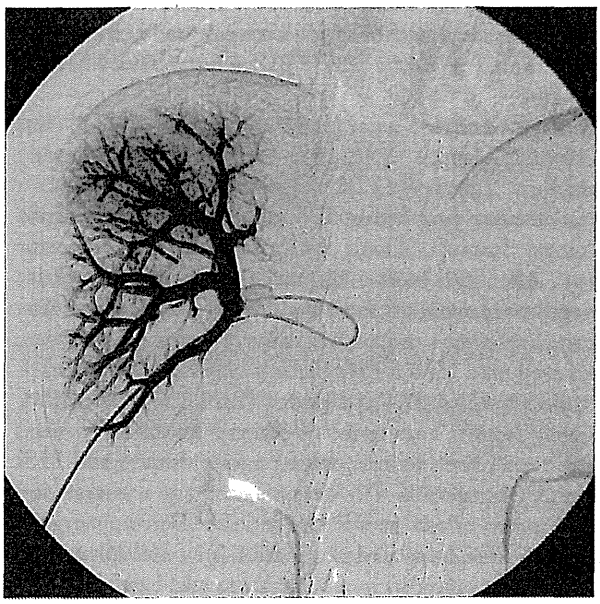

c Balloon occlusion before ethanol injection, right posterior view

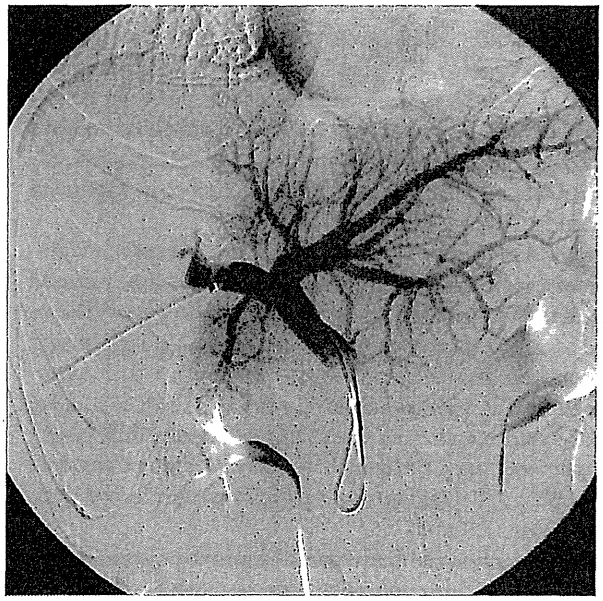

d After portal vein embolization

Fig. 1 Images from a 60-year-old man with gallbladder cancer: **a** anteroposterior portogram obtained before embolization of the right portal venous branches through a 5-Fr angiographic pigtail catheter in the main portal trunk; **b** selective right anterior portogram with balloon occlusion before injection of absolute ethanol; **c** selective right posterior portogram with balloon occlusion before injection of absolute ethanol; and **d** anteroposterior portogram obtained after embolization of the right portal venous branches

dissemination was evident at surgery, surgical resection was not undertaken. Postoperative monitoring was performed daily by the surgeons.

Study endpoints and definitions

The endpoints of this study were: technical success and complications following PVE; changes in serum levels of liver enzymes; changes in FLR and FLR/total functional liver volume ratio; and complications following hepatic resection. Results were also compared with data published in literature on FLR after PVE using other embolic materials.

Statistical analysis

Changes in serum levels of liver enzymes, FLR and FLR/total functional liver volume ratio before and after PVE were compared by means of the Wilcoxon signed rank test. For all tests, $P < 0{\cdot}050$ was considered statistically significant. Statistical analyses were done using the software package SPSS® for Windows® version 12.0 (IBM, Armonk, New York, USA).

Results

A total of 83 patients (53 men and 30 women) with a mean age of 68 (range 45–82) years were included in this study. The primary cancers were: hilar cholangiocarcinoma in 37 patients, colorectal liver metastases in 14, gallbladder cancer in 13, intrahepatic cholangiocellular carcinoma in ten and HCC in nine. Thirteen patients had underlying chronic liver disease (hepatitis B-induced in 7 and hepatitis C-induced in 6). Of these 13 patients, eight had chronic hepatitis and five had liver cirrhosis. Nine patients had diabetes mellitus. Forty-three patients had biliary obstruction and underwent percutaneous or endoscopic biliary drainage before PVE; 15 of these patients were still jaundiced at the time of PVE. Of the 43 patients who underwent biliary drainage, 34 had residual segmental biliary obstruction. The remaining nine patients underwent biliary drainage of the whole liver. None of the patients had undergone chemotherapy or transarterial chemoembolization previously.

In six of the 83 patients, the FLR was larger than 40 per cent, but the surgeon requested PVE to increase the FLR because of older age (3), underlying liver disease (2) or diabetes (1). The planned hepatic resection procedures were right hepatectomy extended to segment IV in 56 patients, right hepatectomy in 24 and right hepatic trisectionectomy in three.

Technical success and complications of the procedure

PVE was technically successful in all patients. The right anterior portal vein was usually used as access (69) but, if necessary, the right posterior portal vein was selected (14). In two patients, it was necessary to embolize intrahepatic portovenous shunts connecting segment VIII branches to a right hepatic venous branch with microcoils, to avoid overflow of absolute ethanol into the systemic circulation. The median total volume of absolute ethanol used was 14 (range 9–25) ml.

Abdominal pain immediately after ethanol injection was common, but disappeared in minutes without treatment or with intravenous pentazocine. Complications related to the procedure occurred in four (5 per cent) of 83 patients, including liver abscess (2), inadvertent thrombosis of the left main portal vein (1) and pseudoaneurysm of the right hepatic artery (1). None of the patients died, and no complications precluded hepatic resection.

Two patients developed a liver abscess in the right lobe and these were treated successfully by percutaneous drainage 11 and 17 days after PVE. These patients were jaundiced at the time of PVE despite percutaneous transhepatic biliary drainage. Sufficient FLR hypertrophy was achieved, and extended right hepatectomy was performed 35 and 30 days after the PVE in these patients.

The inadvertent left main portal vein thrombosis was treated by thrombolysis and angioplasty, but residual thrombosis persisted. Transient hepatic failure developed and resolved in 20 days. Sufficient FLR hypertrophy was achieved, and right hepatectomy was undertaken 27 days after PVE.

Pseudoaneurysm of the right hepatic artery was found in one patient on Doppler ultrasonography 1 day after PVE and was treated successfully by percutaneous thrombin injection.

Changes in serum liver enzyme levels

Serum levels of liver enzymes increased dramatically on the first day after PVE, and then decreased gradually towards the time of hepatic resection (*Table 1*). A median of 20 (range 14–30) days after PVE, levels were no different from those before embolization.

Changes in liver volumes

CT volumetric data showed that mean(s.d.) total functional liver volume before embolization and a median of 17 (range 12–37) days after PVE were 1163(195) and 1159(165) cm^3 respectively (*Table 2*). Mean FLR and mean

Table 1 Serum liver enzyme levels before and after right portal vein embolization

	Before right PVE	1 day after right PVE	Just before hepatic resection	*P**
AST (units/l)	46(30) (13–159)	451(413) (105–2198)	43(18) (15–95)	0·170
ALT (units/l)	60(59) (8–319)	394(342) (79–1126)	53(28) (12–138)	0·109
LDH (units/l)	236(292) (125–2502)	591(463) (203–3105)	240(234) (121–1900)	0·414
ALP (units/l)	586(465) (175–4092)	715(610) (211–4401)	585(350) (198–4017)	0·623
Total bilirubin (mg/dl)	1·34(1·35) (0·4–7·2)	1·95(1·43) (0·6–8·2)	1·09(0·54) (0·4–4·7)	0·062

Values are mean(s.d.) (range). PVE, portal vein embolization; AST, aspartate aminotransferase; ALT, alanine aminotransferase; LDH, lactate dehydrogenase; ALP, alkaline phosphatase. *Wilcoxon signed rank test (before PVE *versus* just before hepatic resection, a median of 20 days after PVE).

Table 2 Changes in liver volume after right portal vein embolization

	Before right PVE	After right PVE	% change	*P**
Total functional liver volume (cm^3)	1163(195) (886–1589)	1159(165) (969–1582)	0(2) (–2 to 4)	0·261
FLR (cm^3)	366(104) (208–561)	513(1116) (361–644)	40(15) (21–73)	< 0·001
FLR/total functional liver volume ratio (%)	31(6) (21–44)	43(7) (34–52)	12(3) (5–18)	< 0·001

Values are mean(s.d.) (range). PVE, portal vein embolization; FLR, future liver remnant. *Wilcoxon signed rank test (before *versus* a median of 17 days after PVE).

Table 3 Comparison of hypertrophic effect of embolic materials used in portal vein embolization

Embolic material	Reference	Change in FLR (%)	Change in the FLR/total functional liver volume ratio (%)
Gelatin sponge	de Baere *et al.*[1]	33	12
	Imamura *et al.*[18]	31	10
Fibrin glue	Nagino *et al.*[2]	32	10
	Nagino *et al.*[6]	27	10
Cyanoacrylate + Lipiodol®	Denys *et al.*[8]	41	8
	de Baere *et al.*[19]	58	13
Polyvinyl alcohol particles + coils	Madoff *et al.*[9]	41	8
	Covey *et al.*[20]	24	n.a.
Absolute ethanol	Sakuhara *et al.*[17]	35	11
	Present study	40	12

FLR, future liver remnant; n.a., data not available. Lipiodol® (Guerbet, Roissy CdG, France).

FLR/total functional liver volume ratio increased significantly after PVE. The change in FLR induced by PVE and the change in FLR/total functional liver volume ratio were comparable to those obtained using other embolic materials in previous studies (*Table 3*). The rate of volume decrease in the embolized right liver lobe was 18(5) per cent. The changes in FLR and FLR/total functional liver volume ratio for patients with HCC were similar to those for patients with other malignancies (42 and 44 per cent, and 12 and 12 per cent, respectively).

Complications following liver resection

Sixty-nine patients underwent hepatic resection a median of 25 (range 14–55) days after PVE. Fourteen patients (17 per cent) did not undergo resection. This was because of peritoneal dissemination at laparotomy in eight patients, and disease progression evident at follow-up CT after PVE in five. One patient with intrahepatic cholangiocellular carcinoma did not undergo hepatic resection because liver regeneration was insufficient.

Postoperative complications following hepatic resection occurred in 19 (28 per cent) of 69 patients, including bile leak (5), wound infection (4), ascites (3), pancreatic leak (1), ileus (1), subphrenic abscess (1), portal vein thrombosis (1), cardiac failure (1), anastomotic leak of a jejunojejunostomy (1) and transient hepatic failure (1). There were no postoperative deaths.

Discussion

In this study, right PVE with absolute ethanol was technically successful and induced sufficient selective hepatic hypertrophy of the FLR in patients with hepatobiliary malignancy. Complications were rare and liver enzyme levels were only transiently, although greatly, increased. Absolute ethanol is a cheap, readily available, embolic material for PVE, and could be used in the first

stage of staged hepatectomy in patients with hepatobiliary malignancy.

The main advantage of absolute ethanol is its strong embolizing effect. Absolute ethanol causes tissue fixation, sludging of blood cells, and protein denaturation and coagulation. In the present study, PVE was successful in all patients, and recanalization of embolized portal branches was not detected after the procedure. Absolute ethanol can embolize both distal outflow and proximal inflow of portal branches because it diffuses quickly owing to its low density and viscosity[10–13]. Absolute ethanol was infused during balloon occlusion via the ipsilateral approach using reverse-curved catheters in the present study. This prevents reflux of embolic materials into portal branches of the FLR[12,13,17,21], and the ipsilateral approach thus helps avoid injury to the FLR[8,13,21].

The present results showed a 12 per cent increase in the FLR/total functional liver volume ratio at a median of 17 days after PVE. This rate of hypertrophy is sufficient and in keeping with results reported for other embolic materials[1,2,5–9,14–16,21]. A potential explanation is that peripheral vessel occlusion and the cytotoxicity of absolute ethanol prevent development of collateral vessels, and contribute to pronounced FLR hypertrophy[12–14]. Besides, atrophy of the diseased liver segments often occurs in patients with segmental biliary obstruction, and also results in compensatory hypertrophy of the non-diseased liver segments without PVE. In this study, 34 of 83 patients had residual segmental biliary obstruction and this may have affected the hypertrophy rate of the non-embolized liver after PVE[22,23].

A potential drawback of PVE with absolute ethanol is the severity of the injury caused. This is underlined by the appreciable increases in liver enzyme levels 1 day after PVE, although levels had returned to baseline by just before hepatic resection, in keeping with previous reports[10–13,17]. Absolute ethanol causes complete and massive hepatocyte cell destruction, and extensive peribiliary inflammation[11–13]. This should be taken into consideration when it is used for PVE. Two patients with jaundice developed liver abscesses after PVE, as reported by others[14–16]. Thus, absolute ethanol should probably be used judiciously in patients with biliary obstruction who have undergone biliary drainage and/or are still jaundiced.

Another drawback may be the severe abdominal pain frequently observed after administration of absolute ethanol. Lidocaine injection into the target portal vein or routine administration of narcotic analgesics before injection of absolute ethanol may be an appropriate countermeasure[17]. In the present study, hospital stay, and duration of antibiotic prophylaxis and analgesic use after PVE were longer than in previous reports in which other embolic materials were used. This may be due to differences in length of hospital stay between Eastern and Western countries, and the use of absolute ethanol, which is more aggressive than other embolic materials.

This study had several limitations. First, this was a retrospective single-centre non-randomized study. Second, length of hospital stay after PVE, intensive care stay and overall duration of hospital stay were not evaluated. Third, the indication for PVE and the mean FLR/total functional liver volume before PVE (31 per cent) in the present study were different from those in previous reports[14–16]. The initial FLR volume and liver cirrhosis have been shown particularly to influence hypertrophy of the FLR after PVE[19,24]. These may have had an adverse effect on changes in the FLR and the FLR/total functional liver volume ratio. Finally, the higher regeneration rate and potentially increased production of hepatotrophic factors by absolute ethanol may accelerate tumour growth in the non-embolized liver. Significant acceleration of tumour growth has been observed after PVE for HCC and liver metastases in the regenerating liver[9,10,25–27]. Nevertheless, 69 (83 per cent) of 83 patients were able to undergo hepatic resection in the present study, although not all tumour-bearing liver was embolized. This is similar to previous reports[6,9,14–16,26]. The present authors believe that absolute ethanol does not accelerate tumour growth in the non-embolized liver in the interval to liver resection. However, it is uncertain whether absolute ethanol affects long-term survival owing to tumour growth in the remaining liver, including potential risks of subsequent biliary cancer in embolized but unresected liver segments[10,15,21].

Disclosure

The authors declare no conflict of interest.

References

1 de Baere T, Roche A, Vavasseur D, Therasse E, Indushekar S, Elias D *et al.* Portal vein embolization: utility for inducing left hepatic lobe hypertrophy before surgery. *Radiology* 1993; **188**: 73–77.

2 Nagino M, Nimura Y, Kamiya J, Kondo S, Uesaka K, Kin Y *et al.* Changes in hepatic lobe volume in biliary tract cancer patients after right portal vein embolization. *Hepatology* 1995; **21**: 434–439.

3 Makuuchi M, Thai BL, Takayasu K, Takayama T, Kosuge T, Gunvén P *et al.* Preoperative portal embolization to increase safety of major hepatectomy for hilar bile duct carcinoma: a preliminary report. *Surgery* 1990; **107**: 521–527.

4 de Baere T, Roche A, Elias D, Lasser P, Lagrange C, Bousson V. Preoperative portal vein embolization for extension of hepatectomy indications. *Hepatology* 1996; **24**: 1386–1391.

5 Abdalla EK, Barnett CC, Doherty D, Curley SA, Vauthey JN. Extended hepatectomy in patients with hepatobiliary malignancies with and without preoperative portal vein embolization. *Arch Surg* 2002; **137**: 675–680.

6 Nagino M, Kamiya J, Nishio H, Ebata T, Arai T, Nimura Y. Two hundred forty consecutive portal vein embolizations before extended hepatectomy for biliary cancer: surgical outcome and long-term follow-up. *Ann Surg* 2006; **243**: 364–372.

7 Ribero D, Abdalla EK, Madoff DC, Donadon M, Loyer EM, Vauthey JN. Portal vein embolization before major hepatectomy and its effects on regeneration, resectability and outcome. *Br J Surg* 2007; **94**: 1386–1394.

8 Denys A, Lacombe C, Schneider F, Madoff DC, Doenz F, Qanadli SD *et al.* Portal vein embolization with *N*-butyl cyanoacrylate before partial hepatectomy in patients with hepatocellular carcinoma and underlying cirrhosis or advanced fibrosis. *J Vasc Interv Radiol* 2005; **16**: 1667–1674.

9 Madoff DC, Hicks ME, Abdalla EK, Morris JS, Vauthey JN. Portal vein embolization with polyvinyl alcohol particles and coils in preparation for major liver resection for major liver resection for hepatobiliary malignancy: safety and effectiveness study in 26 patients. *Radiology* 2003; **227**: 251–260.

10 Shimamura T, Nakajima Y, Une Y, Namieno T, Ogasawara K, Yamashita K *et al.* Efficacy and safety of preoperative percutaneous transhepatic portal embolization with absolute ethanol: a clinical study. *Surgery* 1997; **121**: 135–141.

11 Yamakado K, Takeda K, Nishide Y, Jin J, Matsumura A, Hirano T *et al.* Portal vein embolization with steel coils and absolute ethanol: a comparative experimental study with canine liver. *Hepatology* 1995; **22**: 1812–1818.

12 Ogasawara K, Uchino J, Une Y, Fujioka Y. Selective portal vein embolization with absolute ethanol induces hepatic hypertrophy and makes more extensive hepatectomy possible. *Hepatology* 1996; **23**: 338–345.

13 Satake M, Tateishi U, Kobayashi T, Murata S, Kumazaki T. Percutaneous transhepatic portal vein embolization: effectiveness of absolute ethanol infusion with balloon catheter in a pig model. *Acta Radiol* 2005; **46**: 344–352.

14 Abdalla EK, Hicks ME, Vauthey JN. Portal vein embolization: rationale, technique and future prospects. *Br J Surg* 2001; **88**: 165–175.

15 Abulkhir A, Limongelli P, Healey AJ, Damrah O, Tait P, Jackson J *et al.* Preoperative portal vein embolization for major liver resection: a meta-analysis. *Ann Surg* 2008; **247**: 49–57.

16 van Lienden KP, van den Esschert JW, de Graaf W, Bipat S, Lameris JS, van Gulik TM *et al.* Portal vein embolization before liver resection: a systematic review. *Cardiovasc Intervent Radiol* 2013; **36**: 25–34.

17 Sakuhara Y, Abo D, Hasegawa Y, Shimizu T, Kamiyama T, Hirano S *et al.* Preoperative percutaneous transhepatic portal vein embolization with ethanol injection. *AJR Am J Roentgenol* 2012; **198**: 914–922.

18 Imamura H, Shimada R, Kubota M, Matsuyama Y, Nakayama A, Miyagawa S *et al.* Preoperative portal vein embolization: an audit of 84 patients. *Hepatology* 1999; **29**: 1099–1105.

19 de Baere T, Teriitehau C, Deschamps F, Catherine L, Rao P, Hakime A *et al.* Predictive factors for hypertrophy of the future remnant liver after selective portal vein embolization. *Ann Surg Oncol* 2010; **17**: 2081–2089.

20 Covey AM, Brown KT, Jarnagin WR, Brody LA, Schwartz L, Tuorto S *et al.* Combined portal vein embolization and neoadjuvant chemotherapy as a treatment strategy for resectable hepatic colorectal metastases. *Ann Surg* 2008; **247**: 451–455.

21 Ko GY, Sung KB, Yoon HK, Kim JH, Weon YC, Song HY. Preoperative portal vein embolization with a new liquid embolic agent. *Radiology* 2003; **227**: 407–413.

22 de Baere T, Denys A, Paradis V. Comparison of four embolic materials for portal vein embolization: experimental study in pigs. *Eur Radiol* 2009; **19**: 1435–1442.

23 Guiu B, Bize P, Gunthern D, Demartines N, Halkic N, Denys A. Portal vein embolization before right hepatectomy: improved results using *n*-butyl-cyanoacrylate compared to microparticles plus coils. *Cardiovasc Intervent Radiol* 2013; **36**: 1306–1312.

24 de Graaf W, van Lienden KP, van den Esschert JW, Bennink RJ, van Gulik TM. Increase in future remnant liver function after preoperative portal vein embolization. *Br J Surg* 2011; **98**: 825–834.

25 Elias D, de Baere T, Roche A, Ducreux M, Leclere J, Lasser P. During liver regeneration following right portal embolization the growth rate of liver metastases is more rapid than that of the liver parenchyma. *Br J Surg* 1999; **86**: 784–788.

26 Wakabayashi H, Ishimura K, Okano K, Izuishi K, Karasawa Y, Goda F *et al.* Is preoperative portal vein embolization effective in improving prognosis after major hepatic resection in patients with advanced-stage hepatocellular carcinoma? *Cancer* 2001; **92**: 2384–2390.

27 Hoekstra LT, van Lienden KP, Doets A, Busch OR, Gouma DJ, van Gulik TM. Tumor progression after preoperative portal vein embolization. *Ann Surg* 2012; **256**: 812–817.

Ann Surg Oncol (2014) 21:2882–2888
DOI 10.1245/s10434-014-3701-y

Annals of
SURGICAL ONCOLOGY
OFFICIAL JOURNAL OF THE SOCIETY OF SURGICAL ONCOLOGY

ORIGINAL ARTICLE – PANCREATIC TUMORS

Basing Treatment Strategy for Non-functional Pancreatic Neuroendocrine Tumors on Tumor Size

Yoji Kishi, MD, PhD[1], Kazuaki Shimada, MD, PhD[1], Satoshi Nara, MD, PhD[1], Minoru Esaki, MD, PhD[1], Nobuyoshi Hiraoka, MD, PhD[2], and Tomoo Kosuge, MD, PhD[1]

[1]Hepatobiliary and Pancreatic Surgery Division, National Cancer Center Hospital, Tokyo, Japan; [2]Division of Molecular Pathology, National Cancer Center Research Institute, Tokyo, Japan

ABSTRACT

Background. Surgical resection is advocated for all stages of pancreatic neuroendocrine tumors (PNETs); whether small PNETs can be managed by observation alone is controversial.

Methods. The prognoses of patients with non-functional PNET managed by surgical resection or observation alone were retrospectively analyzed. In patients who had undergone resection, correlation of pathologically assessed tumor extension and grade with tumor size were evaluated.

Results. Nineteen patients with PNET of median tumor diameters of 12 mm (range 6–38 mm) were followed up by observation for 19–162 months. Increase of tumor size >20 % occurred in three patients, resulting in 5-year progression-free survival of 83 %, but no distant metastases occurred. Surgical resection was performed in 71 patients. Tumor size correlated with the incidence of lymph node or hepatic metastases, portal vein invasion, and Ki-67 index. None of the 18 patients with a tumor size ≤15 mm developed lymph node or distant metastases, and all these patients survived without recurrence for 5–283 months. The smallest tumor size with lymph node metastases was 19 mm. The 5-year recurrence-free survivals of patients with a tumor size ≤15 mm (100 %) was significantly better than patients with tumor sizes 16–20 mm (86 %), 21–30 mm (71 %), 31–50 mm (83 %), and >50 mm (48 %).

Conclusion. Because PNETs ≤15 mm in size have little risk of metastases or recurrence, careful observation with serial image studies is acceptable. Once the tumor size exceeds 15 mm, the risk of metastases and recurrence increases significantly.

First Received: 4 February 2014;
Published Online: 18 April 2014

Y. Kishi, MD, PhD
e-mail: ykishi-tky@umin.ac.jp

With ongoing developments in imaging modalities over the last few decades, pancreatic neuroendocrine tumors (PNETs), particularly non-functional ones, have been increasingly recognized. One population-based study showed that the incidence has increased more than twofold in the last 16 years[1] and another showed that the incidence of small non-functional PNETs (≤2 cm) has increased more than sevenfold.[2]

Provided the tumor is considered resectable, the current consensus on optimal treatment for PNETs at any stage is surgical resection, because lymph node metastases can occur even in patients with PNETs of <10–20 mm.[2–9] Several studies have validated aggressive resection of advanced disease with portal vein tumor thrombosis or hepatic metastases.[10–13] For non-functional PNETs, irrespective of tumor size, the National Comprehensive Cancer Network guidelines recommend surgical resection, including regional lymph nodes. They state that enucleation or observation are options for small tumors (<10 mm); however, their criteria are unclear.[14] Of note, few studies have reported long-term outcomes of patients with small PNETs managed by careful observation, provided serial imaging shows no or minimal growth.[15,16] Thus, the optimal strategy for small PNETs is controversial.

In our institution, the management policy for patients with PNETs radiologically assessed as ≤10 mm is close observation at 6-monthly intervals.

This study aimed to evaluate whether tumor size reliably predicts the degree of malignancy and can determine treatment strategy for PNETs.

PATIENTS AND METHODS

Patients

A prospectively collected institutional database of patients with pancreatic tumors was reviewed to identify those treated for non-functional PNET by either surgical resection or observation in our institution from October 1981 to September 2013. The diagnosis of PNET was confirmed pathologically in all patients who had undergone surgical resection, whereas in patients whose tumors had not been resected, the diagnosis of PNET was made by Doppler or contrast enhanced ultrasonography (US) and computed tomography (CT). Fine-needle aspiration (FNA) biopsy was not routinely performed.

Treatment Strategies

Our indication for surgical resection for non-functional PNETs is tumor size >10 mm. Small tumors of up to 10 mm are managed by close observation. Because a few patients with PNET >10 mm refused surgical resection, several patients with larger tumors were treated by observation.

The standard surgical procedure was either pancreaticoduodenectomy or distal pancreatectomy with regional lymph node dissection. For small tumors, parenchyma-preserving procedures were considered. For extensive tumors, portal vein resection or total pancreatectomy was considered. For synchronous liver metastases, simultaneous or secondary hepatic resection was performed provided the tumor was considered resectable.

No patient received preoperative or adjuvant chemotherapy. Every patient was followed-up at 6-monthly intervals by US or CT to evaluate recurrence or tumor progression.

Analyses

In patients undergoing observation, initial tumor size and progression-free survival were evaluated. According to response evaluation criteria in solid tumors,[17] tumor progression was defined as an increase of more than 20 % in diameter. In patients who had undergone surgical resection, first, correlations between tumor size and World Health Organization (WHO) grade based on the Ki-67 index,[18] portal vein invasion, lymph node metastases, and hepatic metastases were analyzed. Distribution by stage based on the European Neuroendocrine Tumor Society (ENETS) TNM classification system[19] was also evaluated. Incidence of postoperative morbidity and subsequent complications were assessed. The severity of pancreatic fistula was classified according to the International Study Group of Pancreatic Fistula criteria.[20] In addition, postoperative recurrence-free survival (RFS) according to tumor size and lymph node status was evaluated.

TABLE 1 Profiles and tumor characteristics of patients in the resection and observation groups

Group	Resection ($n = 71$)	Observation ($n = 19$)	p-Value
Age [years; median (range)]	56 (17–89)	62 (27–79)	0.04
Gender (male/female)	32/39	8/11	0.77
VHL [n (%)]	1 (1)	1 (5)	0.38
Tumor size [mm; median (range)]	28 (0–140)	12 (6–33)	<0.01
Arterial enhancement by CT [n (%)]	64 (90)	19 (100)	0.34

All the above data were obtained at the time of initial diagnosis. Tumor size was based on radiological imaging

VHL Von Hippel–Lindau disease, *CT* computed tomography

Statistical Analysis

Continuous data are expressed as the median and range and were assessed by the Mann–Whitney U test or Kruskal–Wallis test. Categorical data were compared by Pearson's χ^2 test or Fisher's exact test as appropriate. Survival curves were constructed by the Kaplan–Meier method and compared by the log-rank test. A p-value less than 0.05 was considered to be statistically significant in all analyses.

RESULTS

Patient Profiles

During the study period, 81 patients underwent surgical resection of PNETs in our institution. Six patients with functional PNET (gastrinoma, 3; insulinoma, 3), three with mixed acinar-endocrine carcinoma, and one with coexisting invasive ductal carcinoma were excluded. The remaining 71 patients were evaluated as the resection group. Their median age at the time of surgery was 56 years (range 17–81); 39 of these patients (55 %) were female. The observation group consisted of 19 patients, whose median age at the time of referral was 62 years (range 32–79); 11 of these (58 %) were female. The resection and observation groups were completely separate. One patient in the resection group had undergone surgery following 5-year observation at another hospital for a PNET that was initially 10 mm in size and had increased to 21 mm. In the remaining 70 patients, the median interval between the date of diagnosis and surgery was 77 days. Profiles of the patients in each group are summarized in

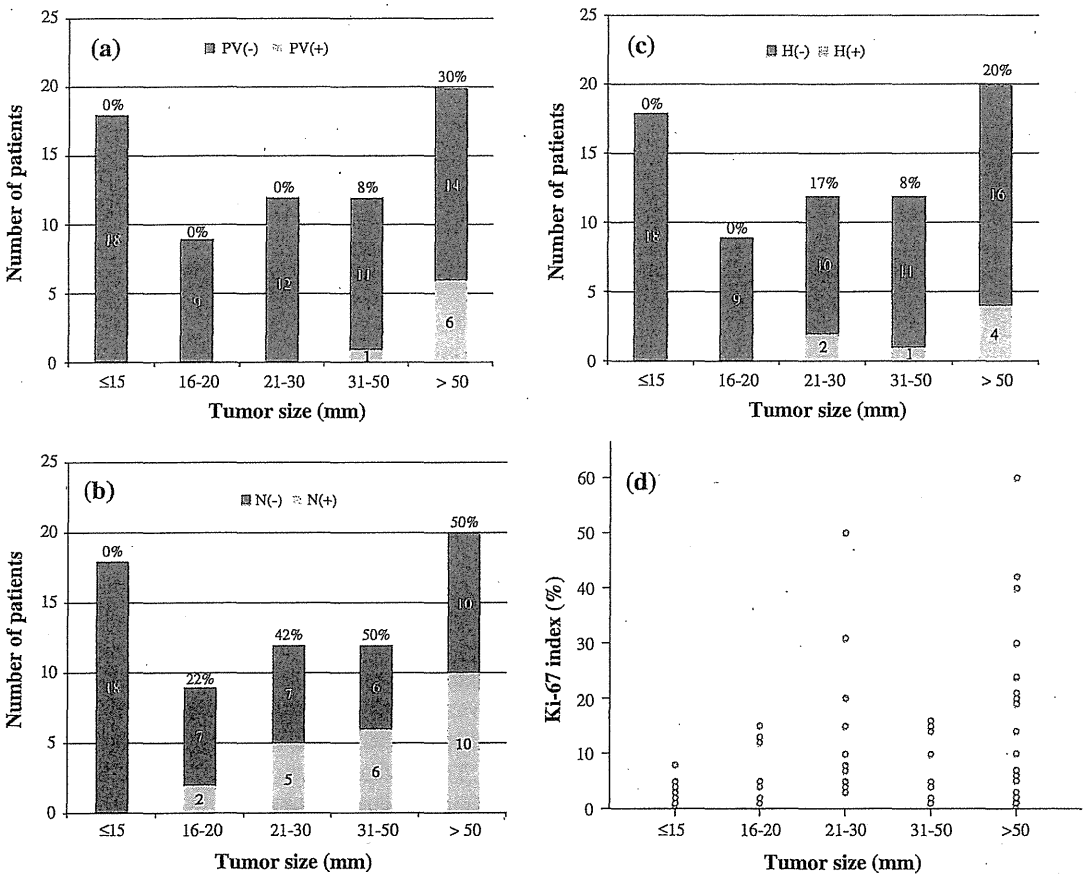

FIG. 1 Incidence according to tumor size of **a** portal vein invasion; **b** lymph node metastases; **c** hepatic metastases. **d** Ki-67 index versus tumor size. The digits above each bar show the positive rates for PV (+), N (+), or H (+). *PV* portal vein invasion, *N* lymph node metastases, *H* hepatic metastases

Table 1. There were two patients with Von Hippel–Lindau disease. All patients had solitary tumors. Tumor size based on CT was significantly larger in the resection group. All tumors in the observation group showed arterial enhancement on CT, but did not in seven patients (10 %) in the resection group. In fact, a definite preoperative diagnosis of PNET was not made in 16 patients in the resection group. The tumors were difficult to differentiate from invasive ductal cancer in eight cases, solid and pseudopapillary neoplasms in four cases, and other tumors (mucinous cystic neoplasm, intraductal papillary mucinous neoplasm, retroperitoneal tumor, metastasis of hepatocellular carcinoma) in four cases.

Prognosis of Patients in the Observation Group

The main reason for observation in patients with tumors of >10 mm was the patients' request. During the median observation period of 45 months (range 19–162), no distant metastases appeared. In any serial image, enlarged lymph node indicating metastasis was not recognized. However, the tumors of three patients increased in size: from 9 to 12 mm in 32 months in one patient, from 10 to 16 mm in 88 months in the second patient, and from 19 to 28 mm in 106 months in the third. Because all three patients refused to undergo surgery, observation was continued. Five-year progression-free survival was 83 %.

Pathologic Findings in the Resection Group

Types of surgical resection were pancreaticoduodenectomy in 31 patients (44 %), distal pancreatectomy in 24 patients (34 %), middle pancreatectomy in 8 patients (11 %), partial resection or enucleation in 5 patients (7 %), and total pancreatectomy in 3 patients (4 %). The total pancreatectomy was performed due to extensive tumor spread along the main pancreatic duct. Seven patients (10 %) had synchronous hepatic metastases, which were resected simultaneously in six patients. In the remaining patient, secondary hepatic resection was planned, but bone metastases were found, prompting abandonment of curative resection.

TABLE 2 Distribution of patients in each ENETS stage according to tumor size

Tumor size (mm)	ENETS stage (%)						Total
	I	IIA	IIB	IIIA	IIIB	IV	
≤15	18 (100)	0	0	0	0	0	18
16–20	3 (33)	4 (44)	0	0	2 (22)	0	9
21–30	0	6 (50)	0	0	3 (25)	3 (25)	12
31–50	0	1 (8)	4 (33)	1 (8)	4 (33)	2 (17)	12
>50	0	0	7 (35)	2 (10)	5 (25)	6 (30)	20
Total	21	11	11	3	14	11	71

ENETS European Neuroendocrine Tumor Society

Figure 1 shows the incidence of portal vein invasion, lymph node metastases, hepatic metastases, and Ki-67 index according to tumor size. There was a tendency for these to be correlated with tumor size. None of the patients with tumors ≤15, ≤20, and ≤30 mm had lymph node metastases, hepatic metastases, and portal vein invasion, respectively. The smallest tumor with lymph node metastasis was 19 mm. All tumors that were WHO grade 3 (corresponding to Ki-67 index >20 %) were larger than 20 mm and the Ki-67 index of all patients with tumors ≤15 mm was less than 10 %.

The numbers of dissected lymph nodes in patients with a tumor size ≤15, 16–20, 21–30, 31–50, and >50 mm were 23 (0–51), 15 (1–37), 17 (1–56), 25 (6–63), and 26 (4–78), respectively, and were comparable among the five groups ($p = 0.37$). No lymph node sampling was performed in four patients, two of whom underwent middle pancreatectomy, one partial resection, and one enucleation for 8–15 mm tumors. The numbers of metastatic lymph nodes in the five groups listed above were 0, 0 (0–2), 0 (0–10), 1 (0–6), and 1 (0–34), respectively. There was a significant difference in the number of metastatic lymph nodes between patients with a tumor size ≤15 and >15 mm ($p < 0.01$), whereas there was no significant difference among the four groups of patients with a tumor size >15 mm ($p = 0.33$). In 64 patients without hepatic metastases, the incidence of lymph node metastases in the five groups was 0/18 (0 %), 2/9 (2 %), 4/10 (40 %), 5/11 (46 %), 7/16 (44 %), respectively. Table 2 shows the distribution of patients of each ENETS stage according to tumor size. All patients with tumors ≤15 mm were classified as stage I, whereas two-thirds of those with PNETs of 16–20 mm were classified as stage II or III.

Postoperative Outcomes and Long-Term Prognosis

Postoperative morbidity occurred in 56 patients (80 %), which was mostly pancreatic fistula in 46 patients (Grade A, 13; Grade B, 32; Grade C, 1[20]) followed by delayed gastric emptying in ten patients. Most of these patients improved conservatively, but arterial bleeding treated by transarterial embolization occurred in one patient. There was no mortality. The median length of stay after surgery was 24 days (12–71). Subsequent complications occurred in 12 patients (17 %) as follows: development of diabetes mellitus, 7 (excluding patients with total pancreatectomy); gastrointestinal bleeding from the anastomotic ulcer, 2; stricture of hepaticojejunostomy required re-anastomosis, 1; stricture of pancreaticojejunostomy, 1; ileus, 1; diarrhea, 1.

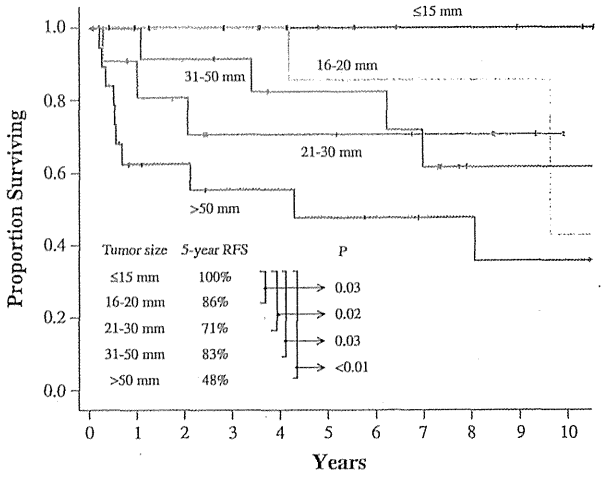

FIG. 2 Postoperative RFS curves according to tumor size. The RFS of patients with tumors ≤15 mm was significantly better than that of any of the other four groups of patients. Differences in RFS among the four groups with tumors >15 mm were not significant ($p = 0.19$). *RFS* recurrence-free survival

During the median postoperative follow-up of 69 months, tumor recurrence was recognized in 19 patients. The site of initial tumor recurrence was most frequently the liver in 14 patients, followed by lymph nodes in two patients, remnant pancreas in one, and bone in one. One had simultaneous liver and lymph node recurrences.

Cumulative 1-, 3-, 5-, and 10-year RFS rates of all 71 patients were 88, 82, 76, and 62 %, respectively. Figure 2 shows the postoperative RFS curves according to tumor size. No patient with tumors ≤15 mm developed recurrence and the RFS for this group was significantly better than for any of the other four groups. The RFS of the four groups of patients with tumors >15 mm did not differ significantly ($p = 0.19$).

DISCUSSION

The present study suggested that small PNETs of up to 10 mm in diameter can be safely observed by serial imaging studies, although the proper size threshold allowing observation could not be determined. It also suggested that the risk of recurrence after surgical resection was significantly lower for PNETs of ≤15 mm than for

TABLE 3 Previous studies concerning lymph node metastases and/or postoperative long-term prognosis of small non-functional PNETs

Authors	Year	N	Tumor size vs. lymph node metastases rate (%)	Prognosis	
				Outcome	Results
Nomura et al.[4]	2009	17	7–15 mm, 0/5 (0) 16–20 mm, 1/2 (50) >20 mm, 5/10 (50)	Postoperative recurrence	7–40 mm ($N = 9$), 0 for 8–120 months >40 mm ($N = 7$), 4 (57 %)
Tsutsumi et al.[7]	2012	59[a]	<10 mm, 0/4 (0) 10–14 mm, 0/18 (0) 15–19 mm, 2/13 (15) 20–29 mm, 1/11 (9) ≥30 mm, 6/13 (46)	NA	
Kim et al.[9]	2012	125	≤10 mm, 0/14 (0) ≤20 mm, 1/51 (2)	Postoperative recurrence	≤10 mm ($N = 14$), 0 ≤20 mm ($N = 51$), 3 (6 %)
Kuo et al.[2]	2013	1371[b]	1–5 mm, 3/12 (25) 6–10 mm, 5/30 (17) 11–15 mm, 14/65 (22) 16–20 mm, 29/80 (36) >20 mm, 494/913 (54)	10-year DSS	1–5 mm ($N = 16$), 100 % 6–10 mm ($N = 51$), 95 % 11–15 mm ($N = 94$), 76 % 16–20 mm ($N = 99$), 76 % >20 mm ($N = 1108$), 59 %
Our study	2014	71	≤15 mm, 0/18 (0) 16–20 mm, 2/9 (22) 21–30 mm, 5/12 (42) 31–50, 6/12 (50) >50 mm, 10/20 (50)	5-year RFS	≤15 mm ($N = 18$), 100 % 16–20 mm ($N = 9$), 86 % 21–30 mm ($N = 12$), 71 % 31–50 mm ($N = 12$), 83 % >50 mm ($N = 20$), 48 %

PNET pancreatic neuroendocrine tumor, *DSS* disease-specific survival, *RFS* recurrence-free survival, *NA* not available

[a] The data excluded patients with gastrinoma but included patients with insulinoma, glucagonoma, and somatostatinoma

[b] Population-level study. Others were all single institutional studies

those >15 mm, for whom the tumor was frequently staged as II or more and the risk of metastases was higher. Not only tumor size, but also tumor differentiation grade, Ki-67 index, and lymph node metastases determine the degree of malignancy and long-term prognosis.[3,6,8,21–24] These studies found that differentiation grade and metastatic status, rather than tumor size, were predictors of prognosis. However, tumor size is usually the only one of these factors that can be assessed by preoperative imaging studies. Although several histopathological studies suggested that intratumoral low microvascular density was associated with poor prognosis,[25,26] arterial tumor enhancement by CT did not discriminate RFS in our series (data were not shown in the results).

So far, no standard strategy for small, non-functional PNETs in particular has been established. Most studies advocate surgical resection for PNETs of any size because even small tumors can be malignant or metastasize to lymph nodes.[2–9,27] Previous studies showing the incidence of lymph node metastases and/or prognosis according to tumor size were summarized in Table 3. Lymph node metastases were recognized even with PNETs of <10 mm. There is a possibility, however, that the incidence of lymph node metastases in patients with small PNETs were overestimated due to the following reasons. First, several studies included functional PNETs such as gastrinoma that frequently involve lymph nodes even with image-negative tiny tumors.[28] In the study by Tsutumi et al., the two patients with node-positive PNET of <10 mm were both gastrinomas.[7] Second, lymph node sampling was not performed in all of the patients. Parekh et al.[27] examined the lymph node status of 149 patients who underwent surgical resection and showed that no lymph nodes were identified in the resected surgical specimens in 43 % of the patients. In our series, the number of lymph nodes sampled did not differ according to the tumor size.

To the best of our knowledge, this is the third reported study (the other two being those of Lee et al.[15] and Gaujoux et al.[16].) that has reported long-term outcomes of patients managed without resection. Although there is a possibility that the diagnosis of PNET in the observation group was inaccurate because no histological confirmation was obtained, not all patients underwent biopsy either in the series by Lee et al. or Gaujoux et al. Our study was similar to theirs in that median tumor size with observation was around 10 mm and tumor

size did not change in most patients throughout the follow-up period. Although the risk of metastases was small, there were some malignant PNETs, especially WHO grade 2 tumors, among tumors ≤15 mm in our resection group; this is in accord with the findings of several previous studies.[2,3,5,9,15] Furthermore, the tumors of several patients in the observation group slowly enlarged; however, no patients in this group underwent resection, even when their tumors had increased in size, because they elected to continue observation. Because none of the 19 patients in the observation group underwent biopsy, the Ki-67 indexes of these patients could not be determined. However, the Ki-67 indexes of the tumors ≤15 mm in the resection group were all less than 10 %. Additionally, the tumor of the one patient who underwent resection because follow-up serial imaging studies showed gradual increase in tumor size had a Ki67-index as low as 3 %. Kim et al.[9] reported that 14 PNETs of ≤10 mm were all WHO grade 1. Lee et al.[15] reported that the Ki-67 indexes of all incidentally identified non-functional PNETs were <5 %, although Ki-67 indexes were available in only 44 % of patients. These results suggest that small tumors of up to around 10 mm are generally low grade.

Considering the risks of pancreatectomy is also important. Usually the pancreas with PNET is soft, associating with high risk of pancreatic fistula, as was suggested from the present results. We further showed the incidence of late-onset complications as 17 %. Previous studies showed the incidence of new-onset diabetes after distal pancreatectomy as 9–36 %.[29,30] Therefore, ideally, pancreatic resection should only be performed in patients with malignant PNETs. Evaluation by FNA may be useful. However, insufficient samples, especially with small tumors,[31] or an adverse event such as pancreatitis,[32] precluded us from routinely performing FNA in all patients with pancreatic tumors, and let us advocate the observation of well-enhanced pancreatic small tumor, although the radiological diagnosis of PNET may be inaccurate.

Limitations of this study include that it was a retrospective study of a small number of patients in both the resection and observation groups. Although, in our series, no metastatic disease or postoperative recurrence occurred in patients with PNETs of ≤15 mm, this group included only 18 patients. To review the previous reports, PNETs less than around 10 mm seem to have a rare risk of recurrence (Table 3). More studies with larger series are required to determine a safe cutoff size for non-operative treatment.

CONCLUSION

Small PNETs of up to around 10 mm can be followed up by careful observation with little risk of tumor progression, while once the tumor size exceeds 15 mm, the risk of metastases and recurrence increase.

ACKNOWLEDGMENT This work was supported by a Grant-in-Aid for Young Scientists (B) [#23791518] from the Ministry of Education, Culture, Sports, Science and Technology of Japan.

REFERENCES

1. Fitzgerald TL, Hickner ZJ, Schmitz M, Kort EJ. Changing incidence of pancreatic neoplasms: a 16-year review of statewide tumor registry. *Pancreas*. 2008;37:134–38.
2. Kuo EJ, Salem RR. Population-level analysis of pancreatic neuroendocrine tumors 2 cm or less in dize. *Ann Surg Oncol*. 2013;20:2815–21.
3. Ferrone CR, Tang LH, Tomlinson J, et al. Determining prognosis in patients with pancreatic endocrine neoplasms: can the WHO classification system be simplified? *J Clin Oncol*. 2007;25:5609–15.
4. Nomura N, Fujii T, Kanazumi N, et al. Nonfunctioning neuroendocrine pancreatic tumors: our experience and management. *J Hepatobiliary Pancreat Surg*. 2009;16:639–47.
5. Haynes AB, Deshpande V, Ingkakul T, et al. Implications of incidentally discovered, nonfunctioning pancreatic endocrine tumors: short-term and long-term patient outcomes. *Arch Surg*. 2011;146:534–8.
6. Hamilton NA, Liu TC, Cavatiao A, et al. Ki-67 predicts disease recurrence and poor prognosis in pancreatic neuroendocrine neoplasms. *Surgery*. 2012;152:107–13.
7. Tsutsumi K, Ohtsuka T, Mori Y, et al. Analysis of lymph node metastasis in pancreatic neuroendocrine tumors (PNETs) based on the tumor size and hormonal production. *J Gastroenterol*. 2012;47:678–85.
8. Krampitz GW, Norton JA, Poultsides GA, Visser BC, Sun L, Jensen RT. Lymph nodes and survival in pancreatic neuroendocrine tumors. *Arch Surg*. 2012;147:820–7.
9. Kim MJ, Choi DW, Choi SH, et al. Surgical strategies for nonfunctioning pancreatic neuroendocrine tumours. *Br J Surg*. 2012;99:1562–8.
10. Norton JA, Kivlen M, Li M, Schneider D, Chuter T, Jensen RT. Morbidity and mortality of aggressive resection in patients with advanced neuroendocrine tumors. *Arch Surg*. 2003;138:859–66.
11. Schurr PG, Strate T, Rese K, et al. Aggressive surgery improves long-term survival in neuroendocrine pancreatic tumors: an institutional experience. *Ann Surg*. 2007;245:273–81.
12. Kleine M, Schrem H, Vondran FW, Krech T, Klempnauer J, Bektas H. Extended surgery for advanced pancreatic endocrine tumours. *Br J Surg*. 2012;99:88–94.
13. Cusati D, Zhang L, Harmsen WS, et al. Metastatic nonfunctioning pancreatic neuroendocrine carcinoma to liver: surgical treatment and outcomes. *J Am Coll Surg*. 2012;215:117–24; discussion 124–5.
14. Neuroendocrine tumors. Version 2. 2414. NCCN Clinical Practice Guidelines in Oncology. http://www.nccn.org/professionals/physician_gls/pdf/neuroendocrine.pdf. Accessed 11 Jan 2014.
15. Lee LC, Grant CS, Salomao DR, et al. Small, nonfunctioning, asymptomatic pancreatic neuroendocrine tumors (PNETs): role for nonoperative management. *Surgery*. 2012;152:965–74.
16. Gaujoux S, Partelli S, Maire F, et al. Observational study of natural history of small sporadic non-functioning pancreatic neuroendocrine tumors. *J Clin Endocrinol Metab*. 2013;98:4784–9.
17. Therasse P, Arbuck SG, Eisenhauer EA, et al. New guidelines to evaluate the response to treatment in solid tumors. European